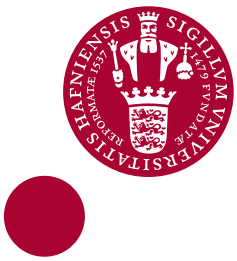

Gap junctions suppress electrical but not [Ca(2+)] heterogeneity in resistance arteries

Hald, Bjørn Olav; Welsh, Donald G; von Holstein-Rathlou, Niels-Henrik; Jacobsen, Jens Christian Brings

Published in:
Biophysical Journal

DOI:
10.1016/j.bpj.2014.09.036

Publication date:
2014

Document version
Early version, also known as pre-print

Article

Gap Junctions Suppress Electrical but Not [Ca^{2+}] Heterogeneity in Resistance Arteries

Bjørn Olav Hald,[1,*] Donald G. Welsh,[2] Niels-Henrik Holstein-Rathlou,[1] and Jens Chr. Brings Jacobsen[1]
[1]Department of Biomedical Sciences, University of Copenhagen, Copenhagen, Denmark; and [2]Department of Physiology & Pharmacology, University of Calgary, Calgary, Alberta, Canada

ABSTRACT Despite stochastic variation in the molecular composition and morphology of individual smooth muscle and endothelial cells, the membrane potential along intact microvessels is remarkably uniform. This is crucial for coordinated vasomotor responses. To investigate how this electrical homogeneity arises, a virtual arteriole was developed that introduces variation in the activities of ion-transport proteins between cells. By varying the level of heterogeneity and subpopulations of gap junctions (GJs), the resulting simulations shows that GJs suppress electrical variation but can only reduce cytosolic [Ca^{2+}] variation. The process of electrical smoothing, however, introduces an energetic cost due to permanent currents, one which is proportional to the level of heterogeneity. This cost is particularly large when electrochemically different endothelial-cell and smooth-muscle-cell layers are coupled. Collectively, we show that homocellular GJs in a passively open state are crucial for electrical uniformity within the given cell layer, but homogenization may be limited by biophysical or energetic constraints. Owing to the ubiquitous presence of ion transport-proteins and cell-cell heterogeneity in biological tissues, these findings generalize across most biological fields.

INTRODUCTION

Cellular heterogeneity is ubiquitous in biological systems (1–3) and hence, is also manifest in the microcirculation (4–7). Individual vascular cells display phenotypic variations due to random events that range from stochastic gene transcription to small fluctuations in the microenvironment. Variability in different properties is routinely documented, e.g., in cellular morphology (3,6,8) or in the activities of ion channels as measured from patch-clamp recordings (Table 1) (data assembled 9–16). Both kinds of variability generate differences in electrical properties between cells within a tissue. The membrane potential (V_m) along the vascular wall, however, is observed to be remarkably uniform (17,18). Also, the passive conduction of electrical signals along the vessel give rise to homogeneous conducted vasomotor responses (5,19,20). The observed variation in basic properties between individual cells on the one hand, and the necessity for synchronized execution of local and conducted vasomotor responses on the other (20–22), raises the intriguing question of how electrical uniformity is achieved.

Vasomotor responses depend heavily on similar extents of activation of voltage-gated Ca^{2+} channels (VGCC) between SMCs. Coordination of activity is mediated by the electrical coupling between neighboring cells which is facilitated by gap junctions (GJs). GJs are hexameric pores of connexin (Cx) protein (Cx subtypes 37, 40, 43, and 45 are found in the vasculature) that, upon docking, allow for direct transfer of ions and small molecules between neighboring cells (21). GJs are highly expressed between endothelial cells (ECs), whereas smooth muscle cells (SMCs) show less pronounced Cx expression (4). Myoendothelial gap junctions (MEGJs) that provide coupling between ECs and SMCs are heterogeneously expressed in different vascular beds (6), although, in general, they are more prevalent in small arterioles (8). We hypothesized that GJs could provide for passive currents between heterogeneous cells that blur the electrochemical differences that would otherwise arise in uncoupled cells. At steady state, however, such passive currents are not free in terms of Gibbs free energy (ΔG_{reac}), i.e., we anticipate a cost in ΔG_{reac} that depends on the level of heterogeneity in the system.

In this article, we employed a modeling approach to examine the influence of GJ distributions on electrical behavior in a heterogeneous cell population. We used well-established computational models for the EC and SMC (23–25). Specifically, we compared steady-state values of V_m, [Ca^{2+}], as well as energetic costs in arterioles that contained the following types of heterogeneity:

1. Ion transport heterogeneity, for which the maximal activity of all ion channels, carriers, and pumps (hereafter summarized as ion transporters) within each EC or SMC was randomly selected from a normal distribution.
2. EC type heterogeneity; the $V_{m,rest}$ of ECs is reported to be relatively heterogeneous; both rather depolarized and hyperpolarized ECs have been found (7,25). Depending on the $V_{m,rest}$ of the SMC layer and the level of MEGJ

Submitted July 10, 2014, and accepted for publication September 30, 2014.
*Correspondence: bohald@sund.ku.dk
Editor: James Sneyd.

0006-3495/14/11/2467/10 $2.00
http://dx.doi.org/10.1016/j.bpj.2014.09.036

TABLE 1 Estimated coefficients of variation in the literature

Ion channel	c [%]	Reference	Ion channel	c [%]	Reference
L-VGCC (Ba^{2+})	26	Harraz and Welsh (9)	K_V	40	Zhong et al. (10)
L-VGCC (Ca^{2+})	120	Rubart et al. (11)	BK_{Ca}	85	Cox et al. (12)
Cl_{Ca}	45	Matchkov et al. (13)	K_{IR}	75	Robertson et al. (14)
NSC	40	Hill et al. (15)	K_{ATP}	25	Kleppisch and Nelson (16)

Maximal conductances were calculated as $g_{max} = I_{max}/(V_m \times C_m)$, where C_m is cell capacitance. Variation coefficients were calculated as $c = \sqrt{n} \times SE(g_{max})/mean(g_{max})$, where n is number of experiments and mean and SE are the average and standard error of measurement, respectively, of g_{max}. In each reference, values were estimated by visual inspection.

coupling, small to large electrical differences between the cell layers may therefore exist. To assess the functional significance of such differences, arterioles were furnished with either a K-type EC layer (predominantly K^+-driven V_m of ~−65 mV) or a Cl^--type EC layer (predominantly Cl^--driven V_m of ~−30 mV).

3. Finally, heterogeneity in MEGJ distributions was introduced by randomly scattering a given number of MEGJs along the arteriole.

Our simulations show that passively open GJs are necessary to homogenize V_m across the arteriole but they cannot eliminate $[Ca^{2+}]$ variation between cells. With MEGJ coupling, the SMC layer is electrophysiologically dominant but coupling is energetically expensive if large endogenous differences in $V_{m,rest}$ is present between cell layers. Heterogenous MEGJ distributions necessitate SMC-SMC coupling to achieve homogeneity in V_m along the SMC layer. In conclusion, GJs are instrumental for the electrical homogeneity that is necessary for synchronous physiological responses across heterogeneous cells in the vascular wall.

MATERIALS AND METHODS

A comprehensive model of a rat resistance arteriole with electrically sealed ends was developed based on previously published electrophysiological models (24,25). Morphology and diffusion was modeled as previously described in Hald et al. (19,23). One layer of ECs is surrounded by one layer of SMCs, oriented perpendicular to the ECs and to the vessel length axis. The modeled vessel is 744-μm long with a diameter of 126 μm and consists of 16 × 6 ECs (circumferential × axial) and 2 × 120 SMCs (Fig. 1). To implement diffusion, each SMC and EC is divided into 8 and 20 segments, respectively (see Section S3 in the Supporting Material). In this model, MEGJ resistance was set to 900 MΩ per SMC. In the case of a nonuniform MEGJ distribution, the MEGJ resistance was scaled to yield 900 MΩ per SMC on average. EC-EC resistance was set to 3 MΩ and SMC-SMC resistance was 90 MΩ (26–28). Gap junctional resistances were converted to permeabilities (24) and these were identical for all ions (i.e., K^+, Na^+, Cl^-, and Ca^{2+}).

Heterogeneity was introduced as follows:

1. Ion transporter and cell volume heterogeneities were introduced by modeling cells with different parameter values, using our previously described modeling strategy (29). Current through every ion transporter is modeled as $I(\mathbf{v}, \mathbf{p}) = a_{max} \cdot f(\mathbf{v}, \mathbf{p})$, where $\mathbf{v}$, $\mathbf{p}$ are variables and parameters, respectively; a_{max} is the maximal activity; and $f(\mathbf{v}, \mathbf{p})$ is an expression that models the kinetics of activation/inactivation. Thus, electrophysiological heterogeneity between cells can be modeled by introduction of variation in a_{max} between cells. Briefly, the a_{max} of all ion transporters in either the EC or SMC (Fig. 1 *A* and see Table S1 in the Supporting Material) was drawn from relevant normal distributions (Fig. 1 *B*), which had an average equal to the value given in Hald et al. (19) and a standard deviation (SD) set to $k \cdot a_{max}$, where $k \in [0.0, 0.1, 0.2]$. Heterogeneity in cell volumes was introduced likewise. The particular sequence of numbers returned by a pseudo-random number generator depends on the seed (see Fig. 1). Therefore, every result obtained is the average of three runs with different seeds.
2. For EC type heterogeneity, the previously published Cl-type EC model (25) has a $V_{m,rest}$ ~−30 mV. To obtain a K-type EC ($V_{m,rest}$ of ~−60 mV), activity of the volume-regulated anion channel (VRAC) was reduced by 90% and the K_{IR}-model activity reduced by 30%, yielding a $V_{m,rest}$ of −65 mV. An endothelium consisting of 50:50 Cl^- and K-types was also constructed by randomly assigning the individual ECs as being of either type.
3. MEGJ heterogeneity was implemented by varying the number and position of EC-SMC connections along the arteriole. The permeability of a single MEGJ was scaled such that the total MEGJ permeability across the arteriole was constant between simulations. In simulations without MEGJ heterogeneity (uniform MEGJ distribution), every segment along the vessel contains a single MEGJ. Each of the 240 SMCs consist of eight segments. The 96 ECs consist of 20 segments each. Thus, the uniform MEGJ distribution has a total of 240 × 8 = 96 × 20 = 1920 MEGJs. With heterogeneity, either 230 or 100 MEGJs, respectively, were distributed randomly between cells of the two layers, i.e., randomly assigned to the 1920 available positions (this is equivalent to roughly 66 and 33%, respectively, of all SMCs harboring one or more MEGJ(s) (see Table S2)). A steady state for each arteriole system was found using the termination criteria described in the Supporting Material (i.e., in strict terms, a pseudo-steady state was found for each system).

Energetic measures of ATPase activity and mean current density were calculated as

$$\text{ATPase} = \bar{I}_{NaK} + \bar{I}_{PMCA}, \quad (1)$$

$$I_{density} = \frac{\sum_i |I_i^{EC}|}{N_{EC} C_{EC}} + \frac{\sum_i |I_i^{SMC}|}{N_{SMC} C_{SMC}}, \quad (2)$$

where $\bar{I}$ denotes the average current of all cells in the given cell layer (EC or SMC). The ATP consumptions of the Na/K exchanger and the plasma-membrane Ca^{2+}exchanger (PMCA) are 1 mol of ATP per mole of charge (2 K^+ and 3 Na^+ are exchanged) moved and 1 mol of ATP per 2 mol of charge (Ca^{2+}) moved, respectively. In $I_{density}$, i denotes every ion transporter in the cell layer, N is the number of cells in the cell layer, and C is the cell capacitance, i.e., we sum up the numerical value of all currents in every cell in the cell layer and divide this sum by the total capacitance of the layer. Because V_m changes relatively little between simulations, the total $I_{density}$ will reflect ΔG_{reac}. The CVODE GM-RES solver (SUNDIALS; Lawrence Livermore National Laboratory, Livermore, CA) (30) was used to solve the system of coupled ordinary differential equations with relative and absolute tolerances of 10^{-4} and 10^{-9}, respectively.

Animal procedures and patch-clamp recordings

Animal procedures were approved by the Animal Care and Use Committee at the University of Calgary. A single female Sprague-Dawley rat was

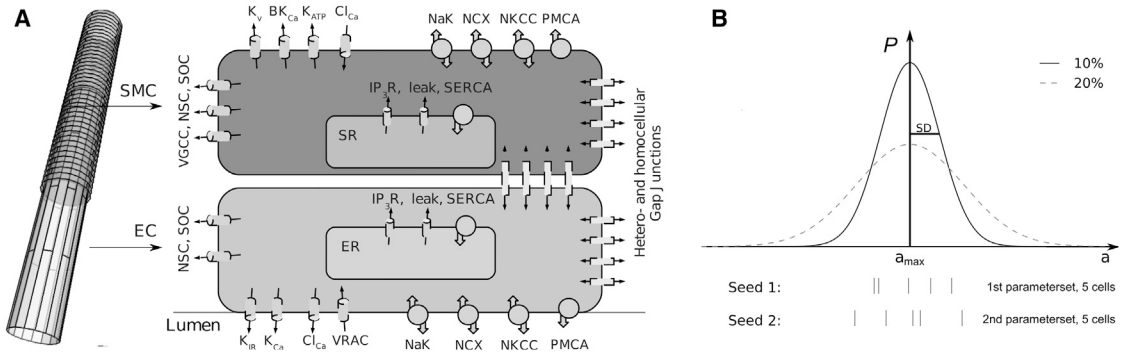

FIGURE 1 Model schematics. (*A*) Morphology and connectivity of a vessel consisting of an EC layer surrounded by one layer of SMCs (*left*); ion channels, carriers, and pumps of each individual EC and SMC (*right*). (*B*) Implementation of heterogeneity in ion transporters between individual cells. The normal maximal activity, a_{max}, of an ion transporter, say PMCA, was set as mean and the SD was set to either 10 or 20% of the mean. A pseudo-random number generator returns sequences of random values from the normal distribution depending on a seed. Seeds 1 and 2 display two hypothetical sequences of five numbers drawn from the normal distribution (position of *vertical bars* represent values of *g*). Each of these values then represent a_{max} of PMCA in five individual cells that now are heterogeneous. (*Solid curve*) Smaller variation with $k = 10\%$; (*dotted shaded line*) Normal distribution with $k = 20\%$.

euthanized by CO_2 asphyxiation and the brain was removed and placed in cold phosphate-buffered (pH 7.4) saline solution containing 138 mM NaCl, 3 mM KCl, 10 mM Na_2HPO_4, 2 mM NaH_2PO_4, 5 mM glucose, 0.1 mM $CaCl_2$, and 0.1 mM $MgSO_4$. After careful dissection of the middle cerebral artery and enzymatical isolation of SMCs, whole-cell currents were recorded using conventional patch-clamp as previously described in Anfinogenova et al. (31). Briefly, borosilicate glass electrodes (Sutter Instruments, Novato, CA), were backfilled with pipette solution: 110 mM K^+-gluconate, 5 mM Na_2ATP, 5 mM HEPES, 0.5 mM $MgCl_2$, 30 mM KCl, 1 mM $CaCl_2$, 0.1 mM GTP, and 4 mM EGTA (pH 7.2, resistance from 5 to 8 MΩ). Only spindle-shaped SMCs with high refraction were patched. GigaOhm seal and plasma membrane rupture were achieved using negative pressure. A holding V_m of −50 mV was applied without pressure for at least 5 min in bath solution: 120 mM NaCl, 3 mM $NaHCO_3$, 1.2 mM KH_2PO_4, 2 mM $MgCl_2$, 10 mM Glucose, 4.2 mM KCl, 1 mM $CaCl_2$, 10 mM HEPES (pH 7.4). Whole-cell currents from isolated SMCs were recorded by voltage-clamping in voltage steps (2 s) ranging from −80 to +10 mV (10-mV intervals), each step followed by a 3 s resting period at −50 mV.

RESULTS

Table 1 illustrates the variation found experimentally in maximal activities of various ion channels across multiple studies. Despite variation being produced by the enzymatic isolation procedure, the relatively large SDs show that heterogeneity in ion channel activity is present between cells. However, variation in total whole-cell current density might be low if the expression pattern of individual ion transporter is regulated, i.e., the activities of ion transporters show high correlation. This is addressed in Fig. 2 showing the variation in whole-cell currents of five individual SMCs obtained from the same enzymatic isolation procedure of a single rat middle cerebral artery. The high SD observed in the depolarized voltage region (where strong outward currents are activated in the SMC) indicates that variation in whole-cell current density between cells is the norm. We conclude that ion transporters display significant (and not fully correlated) heterogeneity in their activities between individual vascular SMCs. However, the extents of true intrinsic differences and artifacts from isolation procedures are impossible to quantify, hence the degrees of intrinsic cellular heterogeneity introduced in the models were chosen to be moderate.

Gap junctions eliminate variation in V_m and reduce variation in $[Ca^{2+}]$

Steady states of arteriolar segments that displayed increasing levels of ion transporter heterogeneity (0, 10, or 20%) were studied in relation to variations in gap junctional subpopulations, i.e., without any coupling (No), with only homocellular GJ coupling (GJ), or with both GJ and

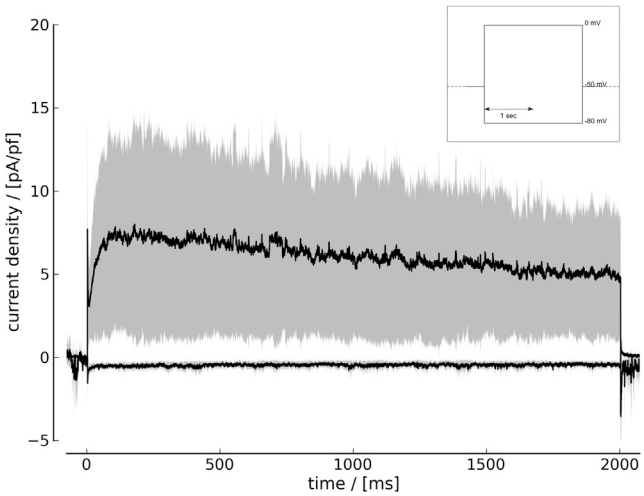

FIGURE 2 Electric current heterogeneity between individual SMCs. Five SMCs isolated from the same middle cerebral artery were patch-clamped in the whole-cell mode to −80 mV (*lower curves*) or 0 mV (*upper curves*) for 2 s and the resulting currents were measured. Holding potential was −50 mV (see *inset* for clamping protocol). (*Solid*) The mean current density of the five measurements; (*shaded*) SD. Only at depolarized potentials are the outward currents large enough to identify substantial heterogeneity.

MEGJ coupling (GJ + MEGJ). To evaluate differences in endogenous $V_{m,\mathrm{rest}}$ of the EC and SMC layers (i.e., V_m difference between uncoupled layers) and how they affected the electrophysiology of the arteriole, arterioles furnished with either K-type ECs or Cl-type ECs were constructed (electrochemical properties are summarized in Table S3). V_m and $[Ca^{2+}]$ characteristics for all permutations are shown in Fig. 3 (see Fig. S1 in the Supporting Material for a 50:50 Cl/K-type arteriole). Fig. 3, *A* and *B*, displays the variation in V_m in arterioles with K-type ECs or Cl-type ECs, respectively. Without coupling (No), significant variation is observed as ion transporter heterogeneity is introduced. However, GJ coupling readily homogenizes any V_m variation within a layer. With MEGJ coupling (900 MΩ per SMC), the two different cell layers attain the same overall V_m. Finally, despite a ΔV_m of ~30 mV between the cell layers before MEGJ coupling in the Cl-type arteriole (Fig. 3 *B*), the SMC layer only depolarizes ~5 mV upon MEGJ coupling, i.e., the electrophysiological activity of the SMC layer is dominating. As seen in Fig. 3 *E*, this homogenization of V_m through MEGJ coupling is produced by a radial steady-state current in the arteriole.

The variation in cytosolic Ca^{2+} concentrations ($[Ca^{2+}]$) in SMCs is surprisingly high upon introduction of ion transporter heterogeneity (Fig. 3, *C* and *D*, *No coupling*) and is only slightly reduced with GJ or GJ + MEGJ coupling. The coefficients of variation (normalized variation) in $[K^+]$, $[Cl^-]$, $[Na^+]$, and $[Ca^{2+}]$ between SMCs at steady state in the K-type arteriole are shown in Table 2 (the same trend is obtained for the Cl-type arteriole, see Table S4). Note that ions present at low concentrations show a large relative variation both with and without coupling. This trend is due to the stoichiometric constraints enforced by many ion transporters, e.g., the $3Na^+/2K^+$ of the Na/K ATPase or the $1Ca^{2+}/2Na^+$ of the NCX exchanger in combination with the numerical spread in concentration of ions. The stoichiometric constraints relay variation in species of high amounts to species of

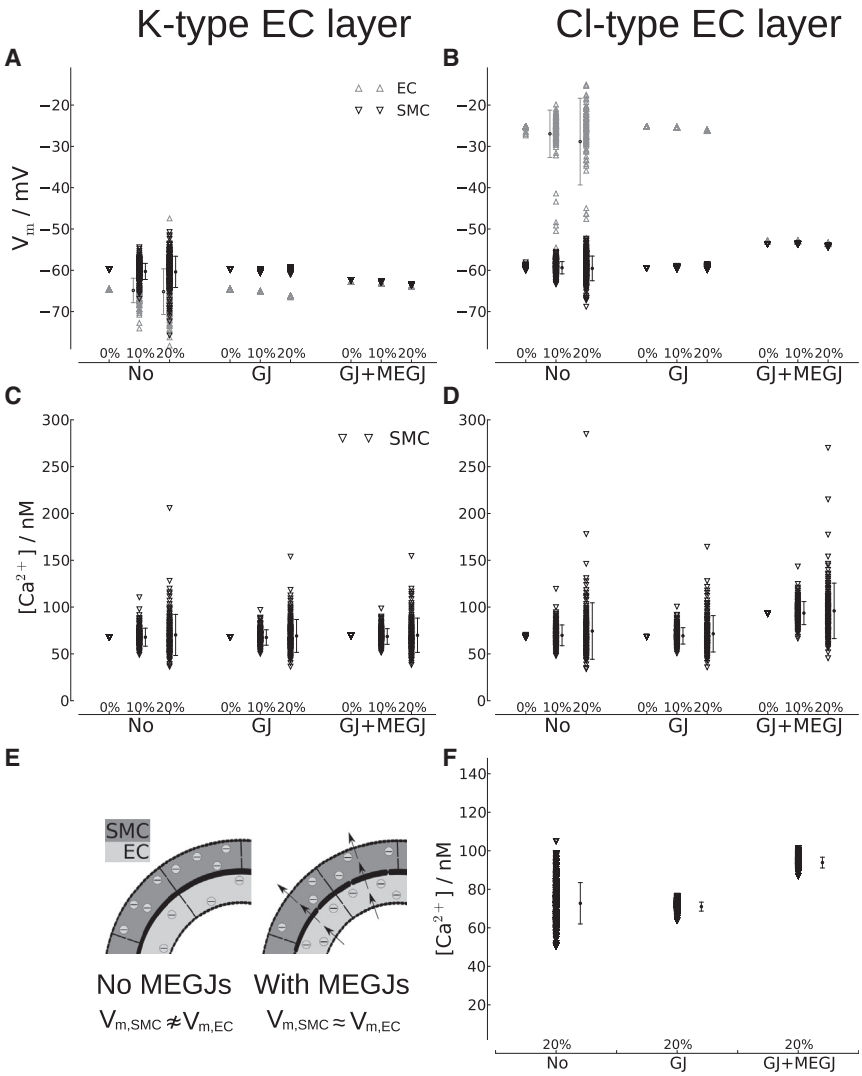

FIGURE 3 Arteriolar V_m and $[Ca^{2+}]$ characteristics at different levels of coupling and ion transporter heterogeneity. Panels *A* and *C* represent K-type models whereas panels *B* and *D* represent Cl-type models, respectively. In each subfigure, the nine columns represent systems with: no coupling (No), only homocellular coupling (GJ), and both GJ and myoendothelial coupling (GJ+MEGJ), permuted with ion transporter heterogeneities of 0, 10, or 20%. (*A* and *B*) Steady-state V_m values of all cells. Where values vary, the mean and SD are also shown. (*C* and *D*) Corresponding variation in $[Ca^{2+}]$. (*E*) Current flows between cell layers with different resting membrane potentials. $V_{m,\mathrm{rest}}$ is determined by ion transporters. With no MEGJ coupling, the two cell layers may have different V_m as indicated by amount of negative charges. With MEGJ coupling, the V_m values of the two cell layers equilibrate at steady state through radial currents. (*F*) $[Ca^{2+}]$ variation in the Cl-type arteriole without heterogeneity in Ca^{2+}-carrying transporters, i.e., identical values of maximal activity parameters described VGCC, NCX, NSK, PMCA, SERCA, SOC, and ER_{leak} (see Table S1 in the Supporting Material) in every cell of the same cell type. Heterogeneity of SD = 20% in the remaining K^+-, Na^+-, and Cl^--transporters (see Table S1) induced electrochemical variation between cells that permeates throughout all variables. Without heterogeneity in Ca^{2+}-carrying transporters, however, $[Ca^{2+}]$ variation is smaller (compare with panels *C* and *D*).

TABLE 2 Coefficient of variation in ionic concentration at steady state

	No			GJ			GJ + MEGJ		
c/mM	0%	10%	20%	0%	10%	20%	0%	10%	20%
$c_{[K+]}$ (144)	0	1	2	0	0	1	0	0	0
$c_{[Cl^-]}$ (65)	0	2	4	0	0	2	0	1	1
$c_{[Na+]}$ (10)	0	8	15	0	5	8	0	4	6
$c_{[Ca2+]}$ (0.070)	0	16	33	0	14	27	0	14	28

The coefficients are defined as $c_X = \sigma_X/\mu_X \times 100\%$, where and σ_X and μ_X are the SD and mean, respectively, of ion [X] among SMCs in the K-type arteriole. "No" refers to no coupling; "GJ" and "GJ + MEGJ" refer to types of coupling; "0%", "10%", and "20%" refer to heterogeneity levels in the maximal ion transporter activities.

low amounts, e.g., from K^+ to Ca^{2+} (Fig. S2 shows that coupling virtually eliminates [K^+] variation). Despite a clear smoothing effect of GJ coupling, the effect is not sufficient to eliminate the variation in low-concentration species that is induced by stoichiometry (compare columns of Table 2).

To highlight that [Ca^{2+}] variation is not just a consequence of heterogeneity in, e.g., VGCC or PMCA, etc., simulations without heterogeneity in any Ca^{2+}-permeable ion channel, carrier, or pump were performed in the Cl-type arteriole. Fig. 3 *F* shows that this situation again leads to variation in [Ca^{2+}] inasmuch as variations in other electrolytes influence [Ca^{2+}] through the stoichiometric constraints of ion exchangers and through the common electrochemical variable, V_m.

Energy consumption increase with electrochemical cell-cell differences

Next, proxies for energetic consumption at steady state were calculated. Fig. 4, *A* and *B*, shows the average ATP consumption (*gray* and *white bars*) in the EC (*gray bar*) and SMC (*white bar*) due to the Na/K ATPase and the PMCA in both types of arterioles. With GJ coupling only, ionic transporter heterogeneity does not affect overall consumption. This is primarily a consequence of the normal distribution being symmetrical. Ionic transporter heterogeneity is, however, evident as cell-to-cell variability (i.e., size of error bar). MEGJ coupling, on the other hand, impacts ATP consumption if the endogenous $\Delta V_{m,\mathrm{rest}}$ between the cell layers is large. In that case (Fig. 4 *B*), a current flows at steady state from the more positive layer to the more negative layer (Fig. 3 *E*). This is a consequence of the steady-state criterion,

$$\frac{dV}{dt} = -\sum_i I_{\mathrm{PM},i}/C_m = 0,$$

where $I_{\mathrm{PM},i}$ denotes all currents across the plasma membrane, and currents flowing through MEGJs.

When this criterion is fulfilled, currents between the layers ultimately have to be compensated for by influx/efflux to/from the extracellular compartment. Although ATP is the energetic currency of a cell, the actual energetic expenditure is not accurately measured through the ATP consumption by the Na/K ATPase and PMCA activities alone. For example, the constant extracellular environment (i.e., constant electrolyte concentrations) provides for more or less constant driving forces across all ionic transporters. The energy required to ensure a constant extracellular medium is afforded elsewhere in the body. Thus, a better, yet still approximate measure of Gibbs free energy expenditure may be obtained by calculating the total flux of current in the arteriole (normalized to the total capacitance of each layer).

Fig. 4, *C* and *D*, shows that increasing the level of ionic transporter heterogeneity indeed increases the total flux, i.e., it increases $|\Delta G_{\mathrm{reac}}/t|$ (t is time), as expected. This increase is due to gap junctional currents (almost no increase is observed without coupling). A large increase in total current flux is observed in the Cl-type arteriole (Fig. 4 *D*), due to the large $V_{m,\mathrm{rest}}$ difference between the two cell layers. The total current flux in this system increased ~75% relative to the segments with no coupling (Fig. 4 *D*). The small V_m difference of the K-type arteriole (Fig. 4 *C*) only increased the total flux between 15 and 30%. The exact flux increase depends on the V_m difference as well as the actual degree of heterogeneity among cells. Despite differences in VRAC and K_{IR} activities leading to different $V_{m,\mathrm{rest}}$ for the two EC types, the two systems do not deviate much in energy consumption in the absence of MEGJs (*GJ* column, Fig. 4, *C* and *D*).

Nonuniform MEGJ distribution necessitates SMC-SMC coupling

In contrast to homocellular GJs, MEGJs are not found in every vascular cell but are nonuniformly distributed along the vascular wall (6). Consequently, we varied the number of MEGJs and inserted them randomly between particular ECs and SMCs. The total MEGJ conductance in the arteriole, however, was the same in all simulations. For clarity, only the Cl-type system was considered (similar results are obtained in the K-type system). Fig. 5 shows V_m distributions at steady state of arterioles with or without homocellular GJs in the SMC layer (GJ^{SMC}) and containing different MEGJ distributions, as follows: 1. A uniform MEGJ distribution (i.e., 100% of SMCs connect to the EC layer), 2. Two-hundred-and-thirty MEGJs (i.e., 66% of randomly chosen SMCs contained MEGJs), and 3. One-hundred MEGJs (i.e., 33% of randomly chosen SMCs contained MEGJs). With homocellular GJs in the SMC layer, no differences in V_m are observed regardless of MEGJ distribution (Fig. 5 *A*). To the contrary, without GJ^{SMC} (Fig. 5 *B*), variability appears in nonuniform MEGJ distributions and the V_m of the two layers did not equilibrate. This highlights that SMC-SMC coupling (although small) is crucial in

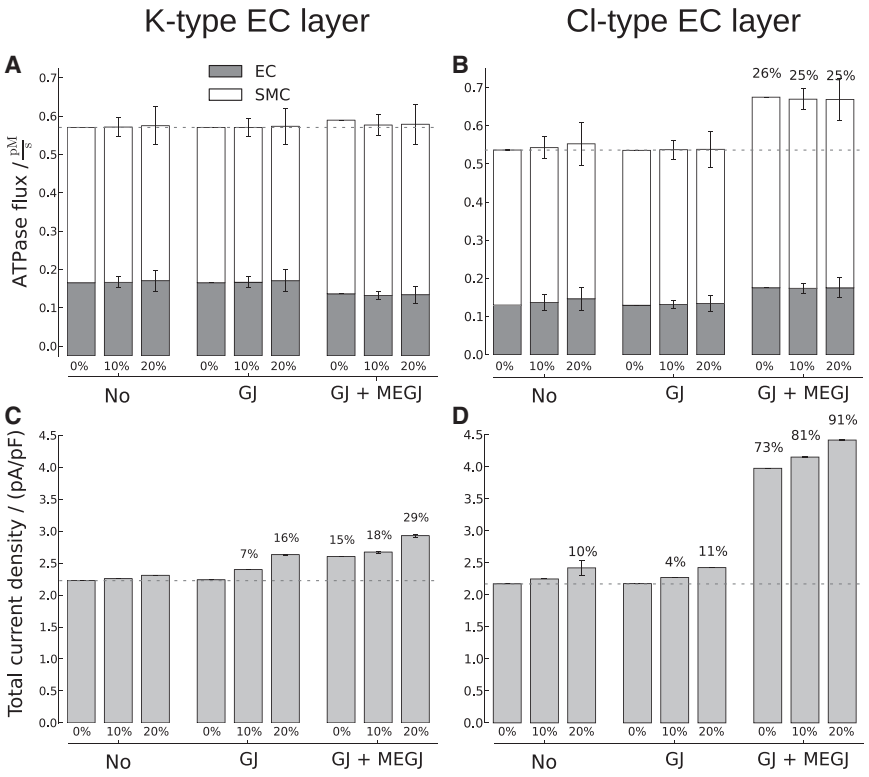

FIGURE 4 MEGJ permeability increases energetic expenditure in vessels with dissimilar endogenous resting potentials. Similar systems as in Fig. 3; however, panels *A* and *B* display the ATP consumption (Na/K ATPase + PMCA per cell) whereas panels *C* and *D* display total current density (normalized sum of all currents) of the corresponding arteriolar systems. Above each bar, the relative increase compared to the first bar (*dashed gray line*, i.e., no heterogeneity and no coupling) is given. (*A* and *B*) Average ATP consumption in an SMC (*white*) placed on top of the ATP consumption in an EC (*gray*). (*C* and *D*) Total current density is displayed.

maintaining a uniform electrical background. However, with all SMCs coupled to the EC layer (100%), GJ^{SMC} is unnecessary for V_m equilibration because of the well-coupled EC layer.

DISCUSSION

In the microvasculature, observations of electrophysiological heterogeneity is a rule rather than an exception (4,7,32). This variation is evident in electrical activity of SMCs (Fig. 2). Inasmuch as electrical uniformity is crucial to execute coordinated vasomotor responses, this study investigates how this uniformity is achieved. Using a modeling approach, both the level of intrinsic ionic transporter variability between cells and cellular coupling can be controlled. The simulations show that passively open homocellular gap junctions are crucial in maintaining a homogeneous electrical background within a heterogeneous cell layer.

However, ions present at low concentrations (importantly Ca^{2+}) show a large relative variation that cannot be homogenized completely by GJs. Connecting the cell layers via MEGJs homogenize membrane potentials across the arteriole and drives the EC potential toward the V_m of the SMC layer. This homogenization, however, is associated with an energetic cost proportional with the electrochemical differences between the layers. Taken together, the study shows that gap junctions, in addition to being pathways for intercellular communication, are essential in mitigating the electrochemical heterogeneity arising from heterogeneity found in multicellular systems (1–3).

Electrical homogenization is crucial for coordinated vasomotor responses

Single cells from the same tissue display heterogeneity in cellular processes (2,3). However, various degrees of intercellular coupling may modulate the electrical heterogeneity observed between individual cells as shown in Fig. 3.

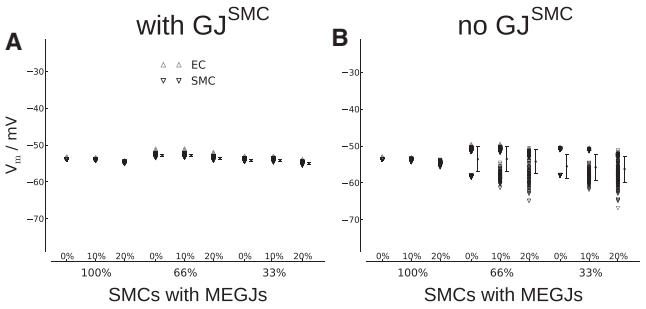

FIGURE 5 SMC-SMC coupling is critical to homogenize V_m in nonuniform MEGJ distributions. The distribution of V_m (*y* axis) in the EC layer (*gray* Δ) and SMC layer (*black* ▽) were assessed in arterioles with different MEGJ distributions corresponding to either 100% (uniform), 66%, or 33% of the SMCs harboring one or more MEGJs and increasing levels of heterogeneity in ionic transporter activities (*x* axis). (*A*) With SMC-SMC coupling (GJ^{SMC}). (*B*) Without GJ^{SMC}. Note that a homogeneous V_m in the SMC layer with nonuniform MEGJ distributions are critically dependent on GJ^{SMC}. Table S2 describes the MEGJ distributions in detail.

Subjecting maximal activities of ionic transporters to be normally distributed with a relatively small SD (10 or 20% of the mean) produces cell-to-cell variability in variables such as V_m and ionic concentrations if cells are uncoupled (see Fig. 3, *A* and *B*). Considering the limited physiological range of membrane potentials in microvessels (~15 to 20 mV (5)), even small differences in V_m of the individual SMCs would produce a variable background for electrical events, most importantly in the activities of voltage-gated ion channels and, in turn, this would lead to variable tone along the vessel axis. Gap junctional coupling is therefore crucial for homogenizing V_m (Fig. 3, *A* and *B*). Note that even without MEGJs, the relatively low SMC-SMC coupling (~90 MΩ) completely eliminates V_m differences in the SMC layer (Fig. 3, *A* and *B*), i.e., a relatively low cell-cell coupling is sufficient for electrical homogenization (but not for long-range conduction of electrical signals (22,28)). Conversely, the predicted electrical variation may be important to consider in relation to pharmacological GJ inhibitors.

Electrical coupling reduce but do not abolish $[Ca^{2+}]$ variation

Heterogeneity in ion transporter activities may partly explain the experimentally observed variability in $[Ca^{2+}]$ between vascular cells (32). The variability in $[Ca^{2+}]$ is reduced but not eliminated by GJ coupling nor by GJ + MEGJ coupling. This residual variability is a consequence of the stoichiometric constraints of ionic transporters that exchanges or transport ions of different concentrations. Most charge within a cell is found as K^+ or Cl^-, whereas $[Ca^{2+}]$ is minuscule, e.g.,

$$Q_{Ca^{2+}}/Q_{K^+} \approx 1.5 \times 10^{-6}.$$

Because a number of important ion exchangers, e.g., the NCX and Na/K ATPase, transport ions in a specific stoichiometric ratio, the variation of the corresponding ions is correlated to some extent. Moreover, heterogeneity in any ionic transporter leads to some variation in $[K^+]$, $[Cl^-]$ or $[Na^+]$ in millimolar ranges, whereas $[Ca^{2+}]$ variation is in the nanomolar range. Hence, during equilibration to steady state, the variation in $[K^+]$, $[Cl^-]$ or $[Na^+]$ is transferred nonlinearly to the much smaller $[Ca^{2+}]$.

The permanent residual $[Ca^{2+}]$ variation imply that global stimuli perturbing the homogenized V_m of the arteriole impact the mean $[Ca^{2+}]$. Being a second-messenger, $[Ca^{2+}]$ is normally very low (~100 nM) and some variability between cells is therefore likely to be insignificant. A depolarizing stimulus induce a high, but probably also rather variable $[Ca^{2+}]$-level between SMCs whereas a hyperpolarizing stimulus decreases $[Ca^{2+}]$. This can only be coordinated among cells if V_m is homogeneous. Therefore, as opposed to variation in V_m, the residual $[Ca^{2+}]$-variability does not preclude coordinated responses in the arteriole. Note, any stimulus that produces a transient change in V_m and/or $[Ca^{2+}]$, e.g., by NO or IP_3 release, cannot homogenize these variables at steady state by definition.

Our model, however, predominantly describes electrical properties of cells. The observed Ca^{2+} variation might be offset (or even reduced) by downstream feedback mechanisms on $[Ca^{2+}]$ that are not captured by the model. In individual cells, for instance, the contractile apparatus is heavily dependent on Ca^{2+}-sensitization (which is independent from electrical events). Small variations in force-generation might be absorbed and capped by the elastic extracellular matrix. Elasticity and nonuniform Ca^{2+}-sensitivity among SMCs might thus be speculated to offset and thereby homogenize the mechanical response.

Energy expenditure increase with heterogeneity and MEGJ coupling

The $V_{m,rest}$ of individual EC has been reported to be heterogeneous even within the same vascular bed (7). Both K- and Cl-type ECs are reported in situ (with K-type ECs being more prevalent in larger vessels) (33). Some studies even report bimodal distributions of $V_{m,rest}$ of both cultured ECs and in vitro (34). The latter findings, however, conflict with the prevalent view that the EC layer is electrically well coupled. Along the same lines, high MEGJ permeability should restrict the V_m difference between EC and SMC layers. To investigate these controversies, we therefore devised different types of models, depending on EC types: only Cl-types or only K-types (Section S2.2 in the Supporting Material also considers a 50:50 split of K- and Cl-types). With MEGJ coupling, the homogenizing effect is evident. Irrespective of EC-type, the endogenous differences in $V_{m,rest}$ of cells within the arteriole are homogenized. Electrophysiologically, the EC layer is dominated by the SMC layer(s), i.e., MEGJ coupling produce marked changes in the V_m (and $[Ca^{2+}]$) of ECs compared to SMCs (see Fig. 3 *A*). This agrees with SMCs being larger, more numerous, and electrophysiologically excitable compared to the underlying ECs.

MEGJ coupling, however, increase energy expenditure, particularly in the presence of a large difference in endogenous $V_{m,rest}$ between cell layers. An ~80% increase in total current flux and ~25% increase in ATP consumption were calculated for the Cl-type arteriole (Fig. 4, *B* and *D*). This is substantial because the energetic expenditure attributed to the NaK exchanger is ~10% in muscle cells (35).The increase in expenditure is due to the directed flow of current from one layer to the other. Ion transporter heterogeneity in itself also causes increased energy expenditure (provided that cells are coupled), but this is only reflected in the total current flux. In this latter case, however, the expenditure is small because the gap junctional currents flow within a layer of similar electrophysiology.

Fig. 3, *A* and *B*, indicates that the electrophysiological dominance of the SMC layer reduces the significance of the particular type of EC (provided that MEGJ coupling is sufficiently high). Yet, the energetic consequences are considerable. Consequently, it seems energetically costly but of physiologically limited significance to have large electrophysiological differences between coupled cell layers. In other words, why expend energy if no change is seen? For a vessel with MEGJ coupling, it could therefore be speculated that the endothelium adapts its ionic transporter composition to match the $V_{m,\mathrm{rest}}$ of the dominant SMC layer. A matching V_m between ECs and SMCs is found in a number of studies (18,33) but is contradictory to other findings (7), where microvascular ECs were depolarized compared to SMCs. However, the latter studies were performed either in cultured cells or in coronary ECs, where MEGJs are absent. The pronounced presence of caveolae and other vesicles along the EC membrane may suggest a capacity for modulation of EC ionic transporter composition. Along the same line, we show in Fig. S1 that an arteriole consisting of 50:50 Cl and K-type ECs also homogenizes in terms of V_m because of the presence of homocellular GJs, suggesting that large differences in electrophysiology within the EC layer are unlikely.

With constant extracellular ionic concentrations and both electrical and $[K^+]$ variability being countered by homogenizing K^+ and Cl^- currents through GJs, the electrochemical gradient overcome by the Na/K ATPase, and thus its ATP consumption, remains fairly constant. However, with MEGJ coupling of cell layers of different electrophysiological properties, the movement of current is directed from the EC layer to the SMC layer (Fig. 3 *E*). The continuous influx/efflux of ions to cells of opposite cell type perturbs ion transporter activities. Consequently, this leads to changes in ATP consumption as seen in Fig. 4 *B*, but not in Fig. 3 *A*, where the electrical differences are small. Although highly speculative, the increase in ATP consumption by the Na/K ATPase (or the activity of some other specific ionic transporter, see Fig. 4 *D*) might be a sensor of electric differences between cell layers, i.e., as the myoendothelial connection develops, the activity of ionic transporters changes. This could provide for an adaptation mechanism, whereby the cell layers can adapt their electrochemical properties to each other to decrease the energetic futility associated with electrochemical differences between coupled cell layers.

Heterogeneity across vessels and species

The basic mechanisms for vascular tone regulation are universal across vascular beds and between vertebrates. Yet, the relative contributions of these mechanisms (e.g., myogenic reactivity, shear stress, Ca^{2+}- and O_2-sensitivity, etc.) as well as mechanical properties differ between vascular beds. The differences are reflected in the particular electrophysiology of a specific arteriole. For instance, arterioles of mesentery, mouse cremaster, or guinea-pig submucosa have $V_{m,\mathrm{rest}}$ of -51.7 ± 1.6 mV ($n = 7$), -27 ± 1 mV ($n = 13$), and -74 ± 1 mV ($n = 17$), respectively (5,36,37). The $V_{m,\mathrm{rest}}$ and ion concentrations are variables that ultimately depend on the ion transporter furnishing of the specific tissue (i.e., our model is specific to rat mesentery). Thus, any (uncorrelated) variation in ion transporter activities will give rise to electrical variation between uncoupled cells, but is eliminated by open GJs, irrespective of the $V_{m,\mathrm{rest}}$. In other words, GJs in a passively open state is likely a general requirement for electrical homogeneity in all electrically active tissues of coupled cells, including the heart, kidney, pancreas, etc. Moreover, the relatively large variation in $[Ca^{2+}]$ is plausibly a general phenomenon because most cells display a large ratio between the major electrolytes ($[K^+]$, $[Cl^-]$ or $[Na^+]$) and $[Ca^{2+}]$ in the cytosol as well as expression of exchangers, e.g., the NCX. Depending on the specific stoichiometric constraints and the ratio between concentrations, the effect may change somewhat between tissues.

General model limitations are described in Hald et al. (19), Kapela et al. (24), and Silva et al. (25), but limitations of our particular study include the following:

1. No hard data exist on differences in maximal activity between individual cells. However, patch-clamp experiments often show considerable variation as grossly estimated in Table 1 and Fig. 2. Although the SD estimate is >20%, some experimental variability may also come from other sources. Thus, we chose two relatively low, yet illustrative, levels of ionic transporter heterogeneity in our simulations.
2. The models are electrical in nature and do not account for biochemical pathways or other kinds of signaling between the cell layers.
3. The steady-state criterion (see Section S1.3 in the Supporting Material) does not ensure a true steady state, inasmuch as a very slow-moving, pseudo-steady state also fulfills the criterion. However, the pseudo-steady state is arguably a reasonable approximation to the physiological system inasmuch as real systems never relax long enough to reach steady state.
4. We choose normal distributions to account for randomness in maximal conductances. This might not be the relevant distribution in all cases. Notably, right-skewed distribution might be more realistic for proteins expressed in low quantities. Also, parameters were drawn from normal distribution with no correlations. This is probably not the case in living systems. Expression of ion transporters within a single cell is likely to be correlated due to, e.g., expression patterns or cell size. This might reduce overall variability.
5. The study considers the effect of gap junctional coupling with constant overall conductance. Very few quantitative

studies on GJ or MEGJ conductance are available (26,27). The limited availability of experimental measurements is a general weakness of the understanding of electrical communication in the microcirculation as such. However, elimination of V_m-differences due to gap junctional coupling seems robust inasmuch as full homogenization is observed in the poorly coupled SMC layer without MEGJ coupling.

6. The EC model used in this study (25) is not validated to the same degree as the SMC model and shows a rather high sensitivity to ionic transporter heterogeneity. To produce the K-type EC, we changed VRAC and K_{IR} conductances as suggested in Nilius et al. (7). However, this is just one way of achieving the reduction in $V_{m,rest}$ characteristic of the K-type EC.
7. The isolation of single cells for patch-clamp by enzymatic dissociation and trituration invariably incur damage, and is likely to account for a significant part of the observed variability.

CONCLUSIONS

Passively open gap junctions have an important role in homogenizing V_m across the arteriole. We believe that this is critical for the execution of consistent vasomotor responses. Intercellular coupling also reduce variation in ionic concentrations induced by differences in ionic transporter activities. Relative variation is inversely related to the concentration of the relevant ion. This partly explains the $[Ca^{2+}]$ variability observed between cells (32). In turn, this suggests a role for local voltage-independent mechanisms in homogenizing the mechanical output. We show that the SMC layer dominates the EC layer electrophysiologically. Thus, MEGJ coupling results in similar membrane potentials of the cell layers despite differences in $V_{m,rest}$ between the uncoupled cell layers and produces energy expenditure by moving current between the cell layers. Consequently, coupled cell layers in the microcirculation are most likely fairly similar in terms of endogenous electrochemical characteristics. This could also suggest the existence of an adaptation mechanism, most likely in the endothelium, to match the V_m of opposing cell layers. Finally, we show that nonuniform MEGJ distributions in the microvasculature necessitates SMC-SMC coupling to homogenize V_m along the SMC layer.

SUPPORTING MATERIAL

Section S1 Methods (S1.1 Heterogeneous Parameters of Ion Carriers, S1.2 MEGJ Distributions Used in the Simulations, S1.3 Steady-State Criterion), Section S2 Results (S2.1 Coefficients of Variation in the Cl-Type Arteriole, S2.2 50:50 Mix of K- and Cl-Type EC Arterioles, S2.3 $[K^+]$ is Homogenized with Homocellular Coupling in All Systems), S3 Mathematical Models (S3.1 Diffusion Models, S3.2 Gap Junctional Current Models, S3.3 EC Ion Channel Current Models, S3.4 Differential Equations, EC, S3.5 SMC Ion Channel Current Models, S3.6 Differential Equations, VSMC), six tables, two figures, and equations, are available at http://www.biophysj.org/biophysj/supplemental/S0006-3495(14)01010-8.

The authors thank Preben Graae Sørensen for use of his computing cluster. The authors confirm that there are no conflicts of interest.

B.O.H. is supported by Arvid Nilssons Fond, and the Danish Council for Independent Research (grant No. DFF-1333-00172). D.G.W. is supported by an operating grant from the Canadian Institute of Health Research.

SUPPORTING CITATIONS

References (38–41) appear in the Supporting Material.

REFERENCES

1. Altschuler, S. J., and L. F. Wu. 2010. Cellular heterogeneity: do differences make a difference? *Cell.* 141:559–563. http://dx.doi.org/10.1016/j.cell.2010.04.033.
2. Snijder, B., R. Sacher, …, L. Pelkmans. 2009. Population context determines cell-to-cell variability in endocytosis and virus infection. *Nature.* 461:520–523. http://dx.doi.org/10.1038/nature08282.
3. Spencer, S. L., S. Gaudet, …, P. K. Sorger. 2009. Non-genetic origins of cell-to-cell variability in TRAIL-induced apoptosis. *Nature.* 459:428–432. http://dx.doi.org/10.1038/nature08012.
4. Hill, C. E., N. Rummery, …, S. L. Sandow. 2002. Heterogeneity in the distribution of vascular gap junctions and connexins: implications for function. *Clin. Exp. Pharmacol. Physiol.* 29:620–625.
5. Wölfle, S. E., D. J. Chaston, …, C. E. Hill. 2011. Non-linear relationship between hyperpolarization and relaxation enables long distance propagation of vasodilatation. *J. Physiol.* 589:2607–2623. http://dx.doi.org/10.1113/jphysiol.2010.202580.
6. Sandow, S. L., D. J. Gzik, and R. M. K. W. Lee. 2009. Arterial internal elastic lamina holes: relationship to function? *J. Anat.* 214:258–266. http://dx.doi.org/10.1111/j.1469–7580.2008.01020.x.
7. Nilius, B., F. Viana, and G. Droogmans. 1997. Ion channels in vascular endothelium. *Annu. Rev. Physiol.* 59:145–170. http://dx.doi.org/10.1146/annurev.physiol.59.1.145.
8. Sandow, S. L., S. Senadheera, …, M. Tare. 2012. Myoendothelial contacts, gap junctions, and microdomains: anatomical links to function? *Microcirculation.* 19:403–415. http://dx.doi.org/10.1111/j.1549–8719.2011.00146.x.
9. Harraz, O. F., and D. G. Welsh. 2013. Protein kinase A regulation of T-type Ca^{2+} channels in rat cerebral arterial smooth muscle. *J. Cell Sci.* 126:2944–2954. http://dx.doi.org/10.1242/jcs.128363.
10. Zhong, X. Z., K. S. Abd-Elrahman, …, W. C. Cole. 2010. Stromatoxin-sensitive, heteromultimeric Kv2.1/Kv9.3 channels contribute to myogenic control of cerebral arterial diameter. *J. Physiol.* 588:4519–4537. http://dx.doi.org/10.1113/jphysiol.2010.196618.
11. Rubart, M., J. B. Patlak, and M. T. Nelson. 1996. Ca^{2+} currents in cerebral artery smooth muscle cells of rat at physiological Ca^{2+} concentrations. *J. Gen. Physiol.* 107:459–472.
12. Cox, R. H., I. Lozinskaya, and N. J. Dietz. 2001. Differences in K^+ current components in mesenteric artery myocytes from WKY and SHR. *Am. J. Hypertens.* 14:897–907.
13. Matchkov, V. V., C. Aalkjaer, and H. Nilsson. 2004. A cyclic GMP-dependent calcium-activated chloride current in smooth-muscle cells from rat mesenteric resistance arteries. *J. Gen. Physiol.* 123:121–134. http://dx.doi.org/10.1085/jgp.200308972.
14. Robertson, B. E., A. D. Bonev, and M. T. Nelson. 1996. Inward rectifier K^+ currents in smooth muscle cells from rat coronary arteries: block by Mg^{2+}, Ca^{2+}, and Ba^{2+}. *Am. J. Physiol.* 271:H696–H705.
15. Hill, A. J., J. M. Hinton, …, A. F. James. 2006. A TRPC-like non-selective cation current activated by α1-adrenoceptors in rat mesenteric

artery smooth muscle cells. *Cell Calcium.* 40:29–40. http://dx.doi.org/10.1016/j.ceca.2006.03.007.

16. Kleppisch, T., and M. T. Nelson. 1995. ATP-sensitive K^+ currents in cerebral arterial smooth muscle: pharmacological and hormonal modulation. *Am. J. Physiol.* 269:H1634–H1640.
17. Welsh, D. G., and S. S. Segal. 1998. Endothelial and smooth muscle cell conduction in arterioles controlling blood flow. *Am. J. Physiol.* 274:H178–H186.
18. Emerson, G. G., and S. S. Segal. 2000. Electrical coupling between endothelial cells and smooth muscle cells in hamster feed arteries: role in vasomotor control. *Circ. Res.* 87:474–479.
19. Hald, B. O., J. C. B. Jacobsen, …, L. J. Jensen. 2012. BKCa and KV channels limit conducted vasomotor responses in rat mesenteric terminal arterioles. *Pflugers Arch.* 463:279–295. http://dx.doi.org/10.1007/s00424–011–1049–8.
20. Emerson, G. G., and S. S. Segal. 2000. Endothelial cell pathway for conduction of hyperpolarization and vasodilation along hamster feed artery. *Circ. Res.* 86:94–100.
21. de Wit, C., and T. M. Griffith. 2010. Connexins and gap junctions in the EDHF phenomenon and conducted vasomotor responses. *Pflugers Arch.* 459:897–914. http://dx.doi.org/10.1007/s00424–010–0830–4.
22. Tran, C. H. T., E. J. Vigmond, …, D. G. Welsh. 2009. Mechanistic basis of differential conduction in skeletal muscle arteries. *J. Physiol.* 587:1301–1318. http://dx.doi.org/10.1113/jphysiol.2008.166017.
23. Hald, B. O., L. J. Jensen, …, J. C. B. Jacobsen. 2012. Applicability of cable theory to vascular conducted responses. *Biophys. J.* 102:1352–1362. http://dx.doi.org/10.1016/j.bpj.2012.01.055.
24. Kapela, A., A. Bezerianos, and N. M. Tsoukias. 2008. A mathematical model of Ca^{2+} dynamics in rat mesenteric smooth muscle cell: agonist and NO stimulation. *J. Theor. Biol.* 253:238–260. http://dx.doi.org/10.1016/j.jtbi.2008.03.004.
25. Silva, H. S., A. Kapela, and N. M. Tsoukias. 2007. A mathematical model of plasma membrane electrophysiology and calcium dynamics in vascular endothelial cells. *Am. J. Physiol. Cell Physiol.* 293:C277–C293. http://dx.doi.org/10.1152/ajpcell.00542.2006.
26. Lidington, D., Y. Ouellette, and K. Tyml. 2000. Endotoxin increases intercellular resistance in microvascular endothelial cells by a tyrosine kinase pathway. *J. Cell. Physiol.* 185:117–125, http://dx.doi.org/3.0.CO;2–7.
27. Yamamoto, Y., M. F. Klemm, …, H. Suzuki. 2001. Intercellular electrical communication among smooth muscle and endothelial cells in guinea-pig mesenteric arterioles. *J. Physiol.* 535:181–195.
28. Diep, H. K., E. J. Vigmond, …, D. G. Welsh. 2005. Defining electrical communication in skeletal muscle resistance arteries: a computational approach. *J. Physiol.* 568:267–281. http://dx.doi.org/10.1113/jphysiol.2005.090233.
29. Hald, B. O., M. Garkier Hendriksen, and P. G. Sørensen. 2013. Programming strategy for efficient modeling of dynamics in a population of heterogeneous cells. *Bioinformatics.* 29:1292–1298. http://dx.doi.org/10.1093/bioinformatics/btt132.
30. Hindmarsh, A. C., P. N. Brown, …, C. S. Woodward. 2005. SUNDIALS: suite of nonlinear and differential/algebraic equation solvers. *ACM Trans. Math. Softw.* 31:363–396.
31. Anfinogenova, Y., S. E. Brett, …, D. G. Welsh. 2011. Do TRPC-like currents and G protein-coupled receptors interact to facilitate myogenic tone development? *Am. J. Physiol. Heart Circ. Physiol.* 301:H1378–H1388. http://dx.doi.org/10.1152/ajpheart.00460.2011.
32. Lee, C.-H., D. Poburko, …, C. van Breemen. 2002. Ca^{2+} oscillations, gradients, and homeostasis in vascular smooth muscle. *Am. J. Physiol. Heart Circ. Physiol.* 282:H1571–H1583. http://dx.doi.org/10.1152/ajpheart.01035.2001.
33. Wölfle, S. E., V. J. Schmidt, …, C. de Wit. 2009. Prominent role of KCa3.1 in endothelium-derived hyperpolarizing factor-type dilations and conducted responses in the microcirculation in vivo. *Cardiovasc. Res.* 82:476–483. http://dx.doi.org/10.1093/cvr/cvp060.
34. Jiang, Z. G., J. Q. Si, …, A. L. Nuttall. 2001. Two resting potential levels regulated by the inward-rectifier potassium channel in the guinea-pig spiral modiolar artery. *J. Physiol.* 537:829–842.
35. Schramm, M., H. G. Klieber, and J. Daut. 1994. The energy expenditure of actomyosin-ATPase, Ca^{2+}-ATPase and Na^+,K^+-ATPase in guinea-pig cardiac ventricular muscle. *J. Physiol.* 481:647–662.
36. Dora, K. A., N. T. Gallagher, …, C. J. Garland. 2008. Modulation of endothelial cell KCa3.1 channels during endothelium-derived hyperpolarizing factor signaling in mesenteric resistance arteries. *Circ. Res.* 102:1247–1255. http://dx.doi.org/10.1161/CIRCRESAHA.108.172379.
37. Thakali, K. M., S. V. Kharade, …, N. J. Rusch. 2010. Intracellular Ca^{2+} silences L-type Ca^{2+} channels in mesenteric veins: mechanism of venous smooth muscle resistance to calcium channel blockers. *Circ. Res.* 106:739–747. http://dx.doi.org/10.1161/CIRCRESAHA.109.206763.
38. Sandow, S. L., R. Looft-Wilson, …, C. E. Hill. 2003. Expression of homocellular and heterocellular gap junctions in hamster arterioles and feed arteries. *Cardiovasc. Res.* 60:643–653.
39. Sandow, S. L., K. Goto, …, C. E. Hill. 2004. Developmental changes in myoendothelial gap junction mediated vasodilator activity in the rat saphenous artery. *J. Physiol.* 556:875–886. http://dx.doi.org/10.1113/jphysiol.2003.058669.
40. Hald, B., M. F. Madsen, …, P. G. Sørensen. 2009. Quantitative evaluation of respiration induced metabolic oscillations in erythrocytes. *Biophys. Chem.* 141:41–48. http://dx.doi.org/10.1016/j.bpc.2008.12.008.
41. Haas, T. L., and B. R. Duling. 1997. Morphology favors an endothelial cell pathway for longitudinal conduction within arterioles. *Microvasc. Res.* 53:113–120. http://dx.doi.org/10.1006/mvre.1996.1999.